

Non-equilibrium surface diffusion in the O/W(110) system

I. Vattulainen^{a,b,1}, J. Merikoski^{a,b,c}, T. Ala-Nissila^{a,b,d}, and
S. C. Ying^b

^a*Research Institute for Theoretical Physics, P.O. Box 9 (Siltavuorenpenger 20 C),
FIN-00014 University of Helsinki, Finland*

^b*Department of Physics, Box 1843, Brown University, Providence, R.I. 02912,
U.S.A.*

^c*Department of Physics, University of Jyväskylä, P.O. Box 35, FIN-40351
Jyväskylä, Finland*

^d*Laboratory of Physics, Tampere University of Technology, P.O. Box 692,
FIN-33101 Tampere, Finland*

Abstract

In this Letter, we present results of an extensive Monte Carlo study of the O/W(110) system under non-equilibrium conditions. We study the mean square displacements and long wavelength density fluctuations of adatoms. From these quantities, we define effective and time-dependent values for the collective and tracer diffusion mobilities. These mobilities reduce to the usual diffusion constants when equilibrium is reached. We discuss our results in view of existing experimental measurements of effective diffusion barriers, and the difficulties associated with interpreting non-equilibrium data.

Key words: Surface diffusion, Growth, Computer simulations, Tungsten, Oxygen

¹ Corresponding author. E-mail: Ilpo.Vattulainen@csc.fi.

1 Introduction

Surface diffusion plays a significant role in many surface phenomena such as epitaxial growth, catalysis, and ordering [1]. These phenomena are interesting both from the point of view of basic research and applied science. Many new experimental techniques [2–4] have been developed for the measurement of surface diffusion either under equilibrium conditions or slight deviations from equilibrium. There is a corresponding increase in our theoretical understanding of this important quantity. Under near equilibrium conditions, the theoretical description of surface diffusion is well established based on the linear response theory by Kubo [5]. Equivalently, the problem can be described by the diffusion equation governing the evolution of the density profile [6]. However, in many non-equilibrium situations such as surface growth, there is no unique way of defining a diffusion constant D . Yet the diffusive motion of the adatoms clearly plays an important role in such processes. In this work, we will introduce the concepts of tracer and collective *mobilities* which characterize the motion of adatoms under non-equilibrium situations. These quantities are defined as generalizations of the usual diffusion constants to which they reduce in the appropriate limits. To study the non-equilibrium mobilities, we have undertaken an extensive Monte Carlo study of the O/W(110) system using a lattice-gas model. We consider the non-equilibrium ordering dynamics of this system after a quench from a totally random initial state to a temperature characterizing an ordered state. We then divide the time scales into slices

according to the decay of the excess energy. In each time slice, we introduce a definition for tracer and collective mobility. These mobilities are then fitted to an Arrhenius form to extract the effective diffusion barriers that are shown to be strongly time-dependent during the ordering process. For comparison, the equilibrium properties have also been determined. We discuss our results in light of the experimental data by Tringides *et al.* [7–10], and consider the difficulties associated with interpreting non-equilibrium measurements.

2 Model and methods

The phase diagram of the O/W(110) system is fairly well determined through a series of experimental studies [9,11,12]. Its main features have also been obtained from theoretical calculations with a lattice-gas Hamiltonian including pair interactions up to fifth neighbors and triplet interactions [13]. We use this lattice-gas Hamiltonian for our present study of non-equilibrium properties of this system through Monte Carlo (MC) simulations. For this work, we focus at the coverage $\theta = 0.45$. At this coverage, the experimental value for the critical temperature of the order-disorder transition is $T_c^{\text{exp}} \approx 710$ K [12]. Above T_c , the adsorbate is in a disordered phase. Below T_c , the system is characterized by an ordered $p(2 \times 1)$ or equivalently the $p(1 \times 2)$ phase. In this work, we study the ordering dynamics of the system by starting from an initial state, which is completely random such as that obtained from random

deposition at low temperatures. The system is then allowed to evolve towards the equilibrium ordered phase at various temperatures ranging from $0.655 T_c$ to $0.893 T_c$. This procedure corresponds to instantaneous heating in an actual experimental situation.

To perform our MC simulations, we chose the transition dynamics algorithm (TDA) [14]. Within TDA the transition rate $w_{i,f}$, from an initial state i with energy E_i to a final state f with energy E_f , is decomposed into two steps by introducing an intermediate state I with energy $E_I = (E_i + E_f)/2 + \Delta$, where the quantity Δ characterizes the activation barrier in the zero coverage limit due to the substrate-adatom interaction. The rate $w_{i,f}$ is then the product of the two rates $w_{i,I}$ and $w_{I,f}$, which are taken to be of the standard Metropolis form [15]. The TDA describes the classical diffusion barrier more realistically than other transition rate algorithms [14,15], in which the effect of the saddle point of the adiabatic surface potential is not taken into account.

For the present study, we chose $\Delta = 0.0437$ eV. This value is believed to be much lower than the true value which should be closer to the experimentally observed barrier of 0.5 to 0.6 eV [9,16] in the disordered phase. Our choice is necessitated by the need to speed up the jump rate in the numerical simulations at low temperatures. We have done some tests and found that the effect of Δ and the adatom-adatom contributions to the diffusion barrier are approximately additive. Therefore the barriers calculated here should be increased by about 0.5 to 0.6 eV for comparison with the experimentally observed values.

To analyse the ordering dynamics in terms of quasi-equilibrium concepts, we have to divide the total ordering period into different time regimes. These slices of time obviously have to be different at different temperatures because of the change in the rate of ordering. For this purpose, we first calculate the time-dependence of the excess energy of the system, namely $E_x(T, t) = E(T, t) - E(T, \infty)$, after an instantaneous quench at time $t = 0$ from a completely random state to a temperature $T < T_c$. Here $E(T, t)$ is the energy of the system at temperature T and time t . We then introduce the normalized excess energy $F(T, t) = E_x(T, t)/E_x(T, 0)$, which has the maximum $F(T, 0) = 1$. The equivalent time regimes at different temperatures are chosen as intervals between times $t_n(T)$ which satisfy $F(T, t_n(T)) = \exp(-n)$, where the integer $n \geq 0$. Typically, we have used five such time slices here.

Now we come to the definition of the non-equilibrium mobilities. In the case of tracer mobility, we consider the quantity

$$\xi_{\alpha\alpha}^{(n)}(\delta t) = \frac{1}{4N} \sum_{k=1}^N \langle |R_{\alpha}^k(t_n(T) + \delta t) - R_{\alpha}^k(t_n(T))|^2 \rangle, \quad (1)$$

where $\alpha = x, y$ and the sum is over N particles to improve statistics. The two independent spatial components (x, y) of the position vector $\vec{R}^k(t)$ for a particle k at time t are denoted by $R_{\alpha}^k(t)$, i.e. $\vec{R}^k(t) = (R_x^k(t), R_y^k(t))$, and $\langle \rangle$ is used to denote configuration averaging. Within each slice of time, the time difference δt obeys $0 \leq \delta t < t_{n+1}(T) - t_n(T)$. The tracer mobility $D_{T,\alpha\alpha}^{(n)}$ is then defined as the effective slope of $\xi_{\alpha\alpha}^{(n)}$ within the given time regime n . In

equilibrium and for $\delta t \rightarrow \infty$, Eq. (1) is just the tracer diffusion constant D_T times δt . If the system approaches equilibrium as a function of time, $\xi^{(n)}/\delta t$ tends towards D_T , too.

To study collective mobility, we introduce the time-dependent density-fluctuation autocorrelation function

$$S^{(n)}(\vec{R}, \vec{R}', \delta t) = \langle \delta\rho(\vec{R}, t_n(T) + \delta t) \delta\rho(\vec{R}', t_n(T)) \rangle, \quad (2)$$

where \vec{R} and \vec{R}' denote position vectors on a lattice, and the density fluctuations are given by $\delta\rho(\vec{R}, t) = \rho(\vec{R}, t) - \langle \rho(\vec{R}, t) \rangle$. Again, $0 \leq \delta t < t_{n+1}(T) - t_n(T)$ within each time regime n . In the limit of long times (large n and δt) and in the hydrodynamic regime, i.e. in equilibrium, the Fourier transform of this correlation function decays as $S(\vec{k}, \delta t) = S(\vec{k}, 0) \exp(-\vec{k} \cdot D \cdot \vec{k} \delta t)$. In the non-equilibrium situation, we consider $\log S^{(n)}(\vec{k}, \delta t)$ over the given regime n and define its effective slope divided by k^2 as the collective mobility $D_{C,\alpha\alpha}^{(n)}$. In practice this method was carried out with separate sine and cosine transforms of the density fluctuations, following the approach in Ref. [17]. A more detailed presentation of the various methods used will be given elsewhere [18].

The MC calculations were carried out in a $M \times M$ lattice, the system size being $M = 30$. Although it is rather small, it is large enough when one is not close to the critical region. The number of independent samples varied between 1000 and 10000.

3 Results and Discussion

We want to examine first the validity of extracting the mobilities from the quantities $\xi_{\alpha\alpha}^{(n)}(\delta t)$ and $\log S^{(n)}(\vec{k}, \delta t)$ by assuming their linear dependence on δt within each time slice. A typical example of the behavior of $\xi_{xx}^{(n)}(\delta t)$ is given in Fig. 1. The deviations from linear behavior are not very large at any time, therefore our definition for $D_T^{(n)}$ is well justified. A similar result is also found for $\log S^{(n)}(\vec{k}, \delta t)$ used to extract $D_C^{(n)}$. Furthermore, it is evident from Figs. 2 (a) and 2 (b) that within each time slice n the temperature dependence of the resulting tracer and collective mobilities are well described by an Arrhenius form $D^{(n)} \sim \exp(-\beta E_A)$, with E_A denoting the effective activation barrier for diffusion. This allows us to determine the time-dependence of E_A during the ordering process. The results for E_A based on the tracer and collective mobilities are shown in Fig. 3. Three interesting features emerge. At early times, the adsorbate is in a disordered configuration and the adatom-adatom interaction contributions to the activation barrier largely cancel out. Thus, E_A is approximately just the intrinsic barrier Δ . At intermediate times, E_A increases rapidly, with the barrier for the tracer mobility always larger than the corresponding one for the collective mobility. Finally, at long times E_A approaches the equilibrium value $E_A^{\text{eq}} = 0.297 \pm 0.008$ eV given by the dashed line. We note that, in the equilibrium, E_A 's for tracer and collective diffusion are indeed equal within error limits.

We now discuss the relevance of our results to some experiments on the O/W(110) system by Tringides *et al.* [7–10]. These authors studied the ordering dynamics of the $p(2 \times 1)$ phase at $\theta \approx 0.5$ following an up-quench in temperature as in our simulation work. They found that the time-dependent average domain size $L(t)$ followed the growth law $L(t) = A(T)t^\phi$ with $\phi \approx 0.28$, where ϕ is the kinetic growth exponent. Using dimensionality arguments, they argued that the prefactor $A(T)$ can be related to an effective diffusion constant D through the relation $A(T) \propto D^\phi$. Thus, the measured temperature dependence of $A(T)$ allows the determination of an effective diffusion barrier \tilde{E}_A . For this they obtained [7,9] the value of $\tilde{E}_A^{\text{exp}} = 0.61 \pm 0.11$ eV in contrast to the equilibrium measurements of Gomer *et al.* [16,19] who obtained $E_A^{\text{exp,eq}} = 1.0 \pm 0.05$ eV at $\theta \approx 0.56$ in the ordered phase. We performed a similar analysis for the ordering process in our simulations. We used $E_x^{-1}(T, t)$ as a measure for $L(t)$ [20] and found that the growth law is valid over a certain period of time only; namely from the end of an initial transient period to the point when the finite size or pinning effects come into play. In our case, we obtain $\phi \approx 0.5$ in the regime corresponding to the time slices $n = 2, 3$. This is illustrated in Fig. 4. We note that at large times, the growth exponent ϕ is not well defined due to finite-size effects that are rather pronounced after the regime $n = 3$. The value of the effective barrier \tilde{E}_A extracted from the relation $A(T) \propto D^\phi$ is 0.192 ± 0.021 eV. Our time-dependent results for E_A based on the mobilities $D_C^{(n)}$ for these intermediate time regimes range between $0.88 \tilde{E}_A$ and $1.1 \tilde{E}_A$. Thus, we conclude that the procedure of using the dimensional

analysis to extract an effective barrier from the prefactor in the power law growth is indeed valid, and it represents the barrier for the dominant diffusion process in that time regime. Concerning the absolute values of the diffusion barriers, we have to add about 0.6 eV to them as discussed earlier to account for our choice of Δ . This brings our results for the effective barrier in the power law growth regime to 0.8 eV and the final equilibrium barrier to 0.9 eV. The equilibrium value is in agreement with the experimental value. Also we see the same that the adatom-adatom contribution is most dominant in the equilibrium ordered phase and the effective barrier measured during the ordering processes has a smaller value than the equilibrium barrier [21,22]. The discrepancies between our calculated value for \tilde{E}_A and the measured value are not too surprising, since $\phi \approx 0.28$ is considerably lower than the value $\phi \approx 0.5$ observed in our simulations. For the one-component $p(2 \times 1)$ phase whose order parameter is not conserved, the theoretically expected value for ϕ is $1/2$ [20]. Experimentally this value has been observed in the O/W(112) system [23], for example. The experimental data for the O/W(110) system in Refs. [7,9] probably belongs to the early time rather than the intermediate time regime, since the maximum mean diameter of the growing domains during the ordering experiments is smaller than six lattice spacings [7,9]. The \tilde{E}_A^{exp} they measure though represents the effective diffusion barrier for a different configuration than the one in the intermediate time regime. The exact cause for the failure of the experiment to reach the $t^{1/2}$ growth regime is still unclear [10].

We believe that in other non-equilibrium methods such as profile evolution techniques, useful information for an effective mobility is also best extracted from an intermediate time regime. Otherwise, the initial behavior with large deviations from equilibrium behavior would yield results difficult to interpret. Unlike the theoretical simulation studies where we can define the intermediate regimes rather precisely, the practical difficulties in actual non-equilibrium measurements would be to identify the proper intermediate time regimes. In the domain ordering dynamics, we have seen that the power law growth regime can be identified for this purpose. For other non-equilibrium situations, it is not clear how to establish experimentally similar criteria.

Acknowledgements

I. V. thanks the Neste Co. Foundation, the Jenny and Antti Wihuri Foundation, and the Finnish Academy of Sciences for support. J. M. is supported by the Academy of Finland and Emil Aaltonen Foundation. This research has also been partially supported by a grant from the office of Naval Research (S. C. Y. and J. M.). Finally, computing resources of the University of Helsinki and the University of Jyväskylä are gratefully acknowledged.

References

- [1] As a general reference see, for example, *Surface Mobilities on Solid Materials: Fundamental Concepts and Applications*, edited by V. T. Binh (New York, Plenum Press, 1981).
- [2] M. Bott, M. Hohage, M. Morgenstern, T. Michely, and G. Comsa, *Phys. Rev. Lett.* **76**, 1304 (1996).
- [3] B. S. Swartzentruber, *Phys. Rev. Lett.* **76**, 459 (1996).
- [4] M. L. Lozano and M. C. Tringides, *Europhys. Lett.* **30**, 537 (1995).
- [5] R. Kubo, *Rep. Prog. Phys.* **29**, 255 (1966).
- [6] R. Gomer, *Rep. Progr. Phys.* **53**, 917 (1990).
- [7] M. C. Tringides, P. K. Wu, and M. G. Lagally, *Phys. Rev. Lett.* **59**, 315 (1987).
- [8] M. G. Lagally and M. C. Tringides, in *Solvay Conference on Surface Science*, edited by F. W. de Wette (Springer-Verlag, Berlin, 1988) p. 181.
- [9] P. K. Wu, M. C. Tringides, and M. G. Lagally, *Phys. Rev. B* **39**, 7595 (1989).
- [10] M. C. Tringides, Chapter 6 in volume 7 of *The Chemical Physics of Solid Surfaces and Heterogeneous Catalysis: Phase Transitions and Adsorbate Restructuring of Metal Surfaces*”, edited by D. A. King and D.P. Woodruff (Elsevier, 1994).
- [11] W. Y. Ching, D. L. Huber, M. G. Lagally, and G.-C. Wang, *Surf. Sci.* **77**, 550 (1978).
- [12] G.-C. Wang, T.-M. Lu, and M. G. Lagally, *J. Chem. Phys.* **69**, 479 (1978).

- [13] D. Sahu, S. C. Ying, and J. M. Kosterlitz, in *The Structure of Surfaces II*, edited by J. F. van der Veen and M. A. van Hove (Springer-Verlag, Berlin, 1988) p. 470.
- [14] T. Ala-Nissila, J. Kjoll, and S. C. Ying, *Phys. Rev. B* **46**, 846 (1992).
- [15] See *Applications of the Monte Carlo Method in Statistical Physics*, edited by K. Binder (Springer-Verlag, Berlin, 1984).
- [16] J.-R. Chen and R. Gomer, *Surf. Sci.* **79**, 413 (1979).
- [17] C. H. Mak, H. C. Andersen, and S. M. George, *J. Chem. Phys.* **88**, 4052 (1988).
- [18] I. Vattulainen, J. Merikoski, T. Ala-Nissila, and S. C. Ying, to be published.
- [19] M. Tringides and R. Gomer, *Surf. Sci.* **155**, 254 (1985).
- [20] H. C. Fogedby and O. G. Mouritsen, *Phys. Rev. B* **37**, 5962 (1988).
- [21] We point out that we are also aware of other non-equilibrium measurements [24,25] that gave $E_A > 1$ eV. Due to the disordered state during the measurements, these results seem rather high compared with Gomer's equilibrium results [16,19], and are possibly due to impurities [8] or reconstruction [6].
- [22] We like to mention that at $\theta \approx 0.68$, a similar ordering experiment has been carried out by Tringides [26]. In this measurement, the quality of the data seems to be better than in previous experiments at $\theta \approx 0.5$ [7,9]. However, since the final equilibrium phase at the end of the ordering process is a coexistence phase of $p(2 \times 1)$ and $p(2 \times 2)$, and the equilibrium barrier in this phase is unknown, we have avoided comparison with this data.

[23] J.-K. Zuo, G.-C. Wang, and T.-M. Lu, Phys. Rev. Lett. **60**, 1053 (1988).

[24] R. Butz and H. Wagner, Surf. Sci. **63**, 448 (1977).

[25] M. Bowker and D. A. King, Surf. Sci. **94**, 564 (1980).

[26] M. C. Tringides, Phys. Rev. Lett. **65**, 1372 (1990).

Fig. 1. Results for $\xi_{xx}^{(n)}(\delta t)$ with five values of n , after a quench at $t = 0$ from a completely random state to $T = 0.714 T_c$. Time difference δt is given in Monte Carlo steps (mcs). In the inner figure, a part of the small time behavior has been magnified. The results for $\xi_{yy}^{(n)}$ (not shown here) are similar.

Fig. 2. (a) Results for the tracer mobilities $D_{T,xx}^{(n)}$ as an Arrhenius plot. In addition to the equilibrium case that is given for the purpose of comparison (stars and dotted line), results up to $n = 4$ are presented. The results for $D_{T,yy}^{(n)}$ (not shown here) are similar. (b) A similar plot in the case of collective mobility $D_{C,xx}^{(n)}$. Due to separate sine and cosine transforms of the density fluctuations, two values for each pair of T and n are given. The results for $D_{C,yy}^{(n)}$ (not shown here) are alike.

Fig. 3. Results for the effective activation energy E_A versus time. Results with five values of n based on the tracer and collective mobility are shown with full squares and open circles, respectively. Error bars are smaller than the size of the symbol for tracer and approximately of the same size for collective mobility. The equilibrium limit $\tilde{E}_A/E_A^{\text{eq}} = 1$ with $E_A^{\text{eq}} = 0.297$ eV is given by the dashed line. The fit for \tilde{E}_A based on the $A(T)$ data is given in the inset. (See text for details.)

Fig. 4. A typical example of the time evolution of E_x^{-1} data at $T = 0.655 T_c$ as a log-log plot. Time is given in Monte Carlo steps (mcs), and the system size used was 120×120 . A reference curve with $\phi = 1/2$ (dotted line) over the regimes $n = 2, 3$ is also given. The kinetic growth exponent ϕ and the $A(T)$ data were evaluated between 6.9 and 8.3 for $\log t$, yielding 0.514 for ϕ .

Figure 1 by Vattulainen et al.

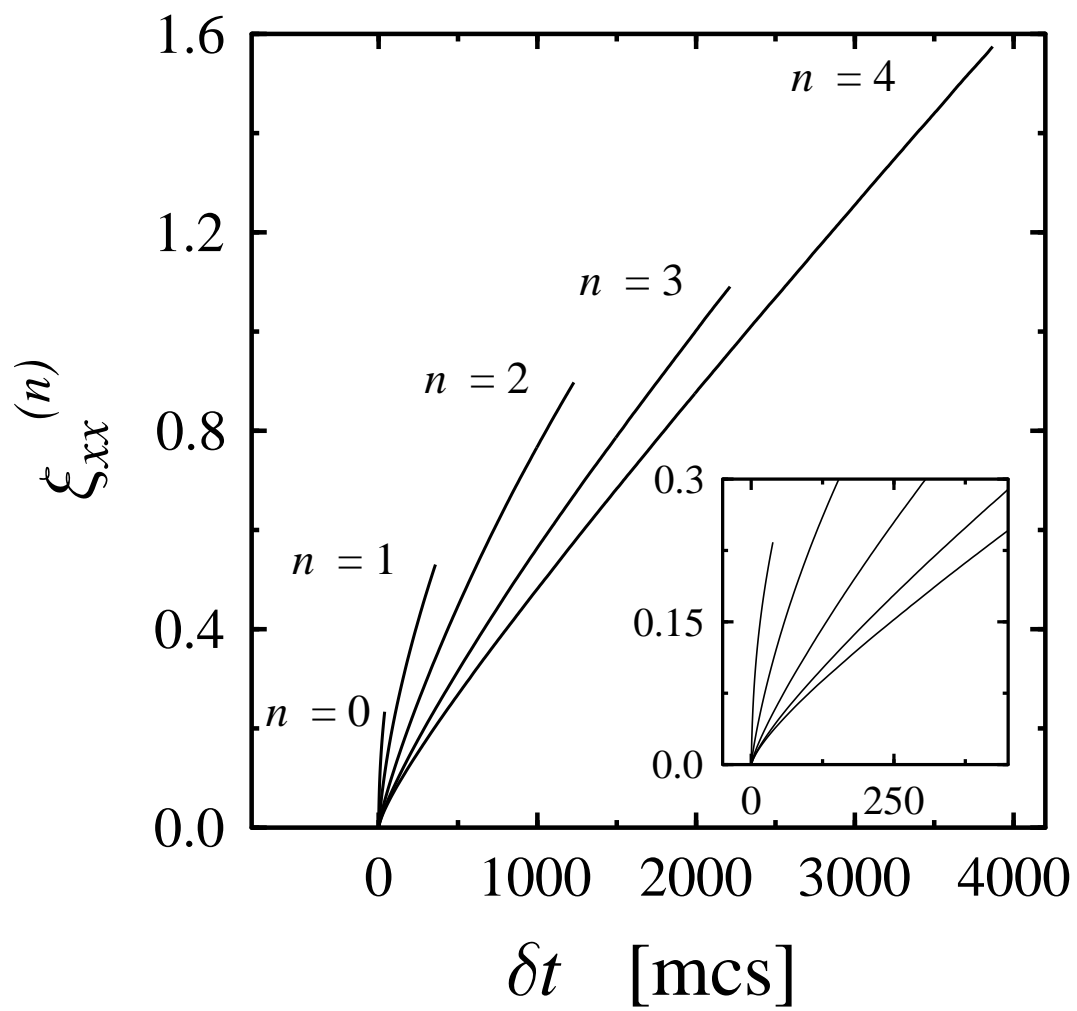


Figure 2 (a) by Vattulainen et al.

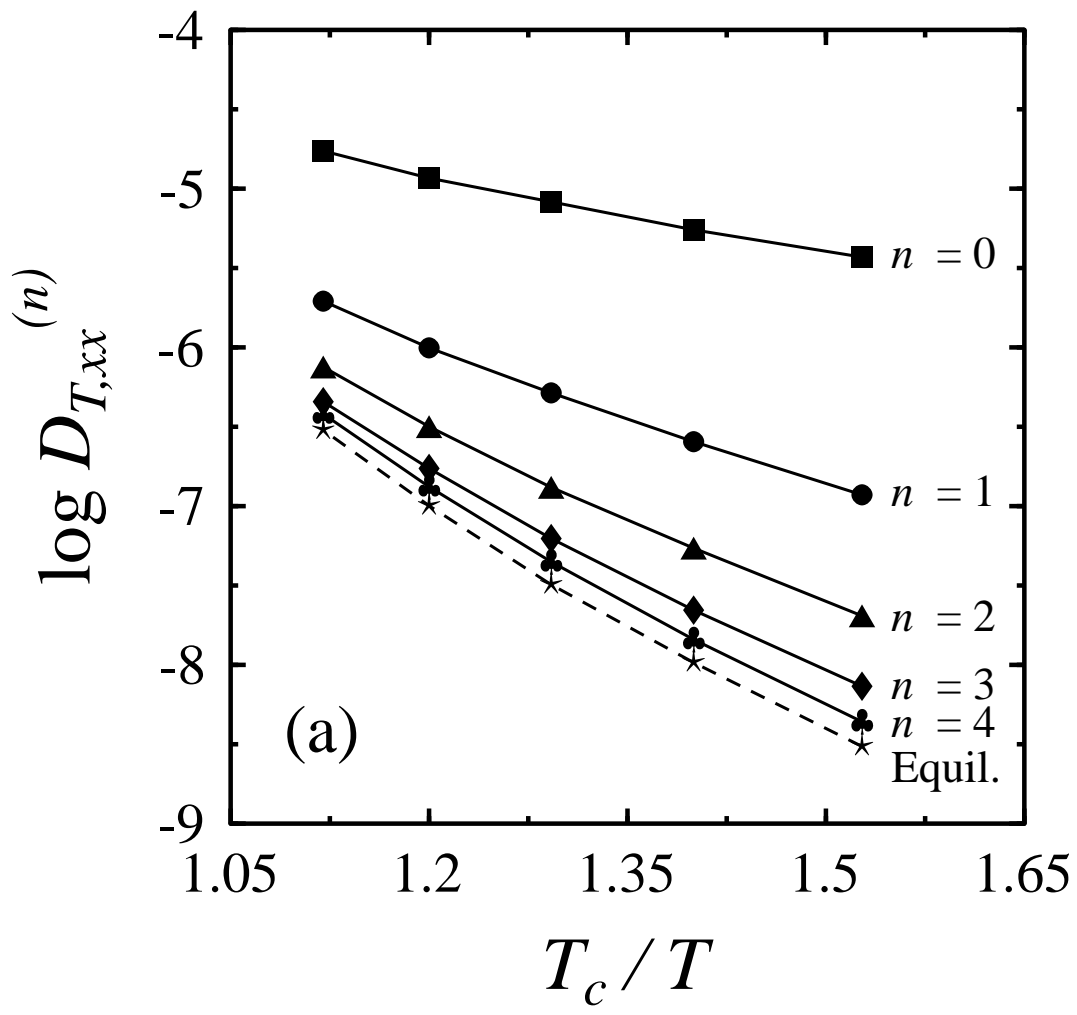


Figure 2 (b) by Vattulainen et al.

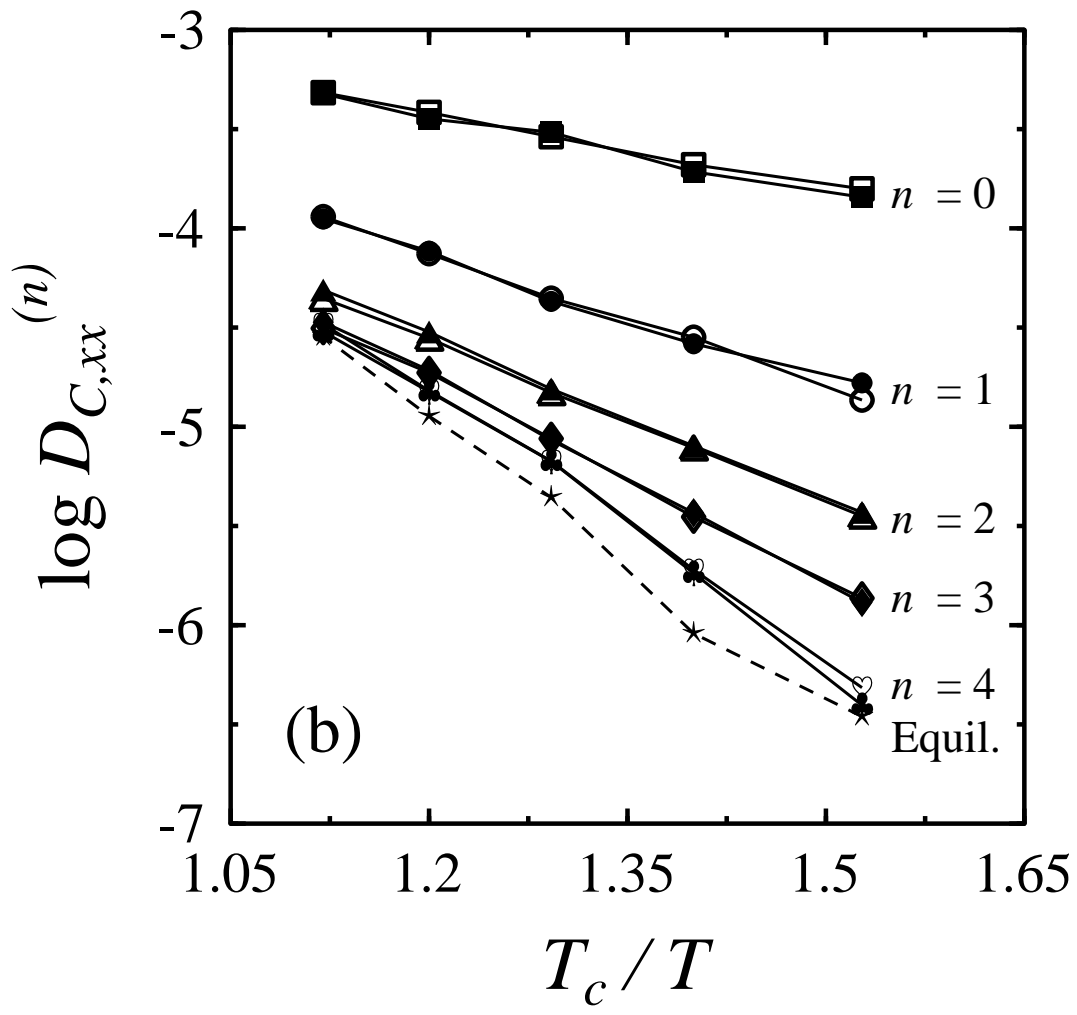


Figure 3 by Vattulainen et al.

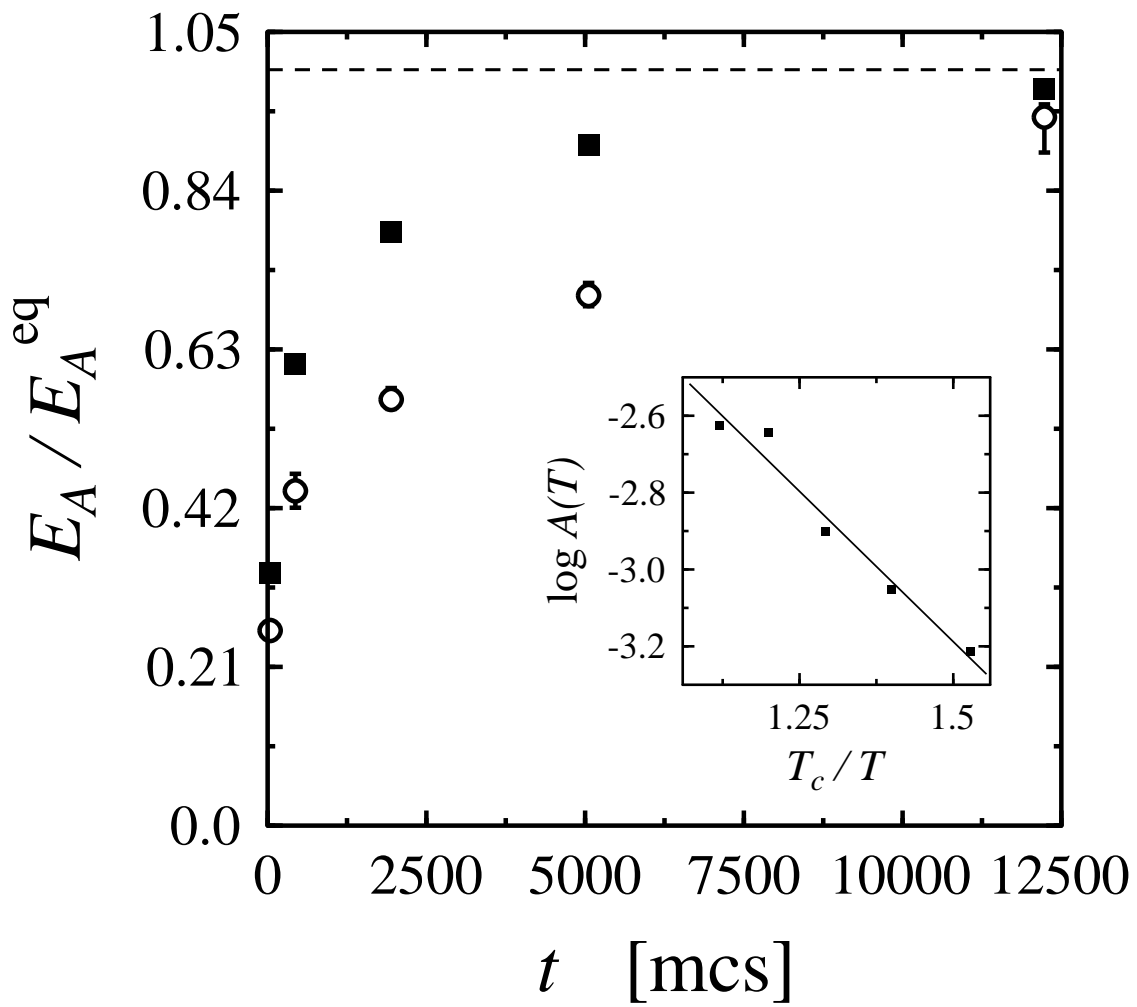


Figure 4 by Vattulainen et al.

